Water Supply

Water Supply Vol 24 No 2, 397 doi: 10.2166/ws.2024.018

Spatiotemporal variation of water balance components in Mashhad catchment, Iran: Investigating the impact of changes in climatic data and land use

Mahdi Zarei [a,*], Reza Ghazavi [b], Khodayar Abdollahi [c], Roberto Ranzi [d], Ramesh S. V. Teegavarapu [e] and Stefano Barontini [d]

[a] Research Center of Social Studies & Geographical Sciences, Hakim Sabzevari University, Sabzevar, Iran
[b] Department of Watershed Management, Faculty of Natural Resources and Earth Sciences, University of Kashan, Kashan, Iran
[c] Faculty of Earth Sciences, Shahrekord University & Board member of Iranian Association of Hydrology, Shahrekord, Iran
[d] Department of Civil, Environmental, Architectural Engineering and Mathematics, University of Brescia, Brescia, Italy
[e] Department of Civil Environmental and Geomatic Engineering, Florida Atlantic University, Florida, USA
*Corresponding author. E-mail: m.zarei@hsu.ac.ir

MZ, 0000-0002-9672-0066; RG, 0000-0002-5487-4710; KA, 0000-0001-7274-0823; RR, 0000-0002-7408-9891; SB, 0000-0001-5967-207X

ABSTRACT

The research aims to investigate the spatiotemporal changes of water balance components and distinguish the relative impacts of climatic data and land-use on groundwater level in northeastern Iran. This investigation employs the WetSpass-M model to estimate water balance and the Mann-Kendall test alongside Sen's slope estimator to evaluate trend. The study also assesses mean annual water balance components, considering diverse combinations of land-use and soil. The findings offer a hydrological insight, revealing that 14% of precipitation results in runoff, 29% of that recharging the aquifer; the remaining portion is lost through evapotranspiration. The trends in precipitation and simulated water components are not significant but a significant downward trend in groundwater is observed beyond a specific point in time. Based on this outcome, as well as the analysis of land-use changes, it was speculated that human activities in this fast-developing region might be implicated in the decline in groundwater levels. Analysis of water balance components in various soil and land-use combinations indicates that evapotranspiration exhibits greater variability within the land-cover class, while recharge is more influenced by soil texture. These findings enhance our understanding for identifying potential sites for artificial recharge and determining sustainable groundwater withdrawals based on spatiotemporal recharge patterns.

Key words: groundwater recharge, Iran, Mashhad Basin, surface runoff, water balance, WetSpass-M model

HIGHLIGHTS

- Groundwater recharge has a higher portion of precipitation than runoff in this arid region which is consistent with some studies in other countries.
- Groundwater level reduction in the study area is more relative to anthropogenic activities than climate.
- Evapotranspiration is more influenced by land use than soil texture.
- Groundwater recharge is more variable within soil texture than within land use.

GRAPHICAL ABSTRACT

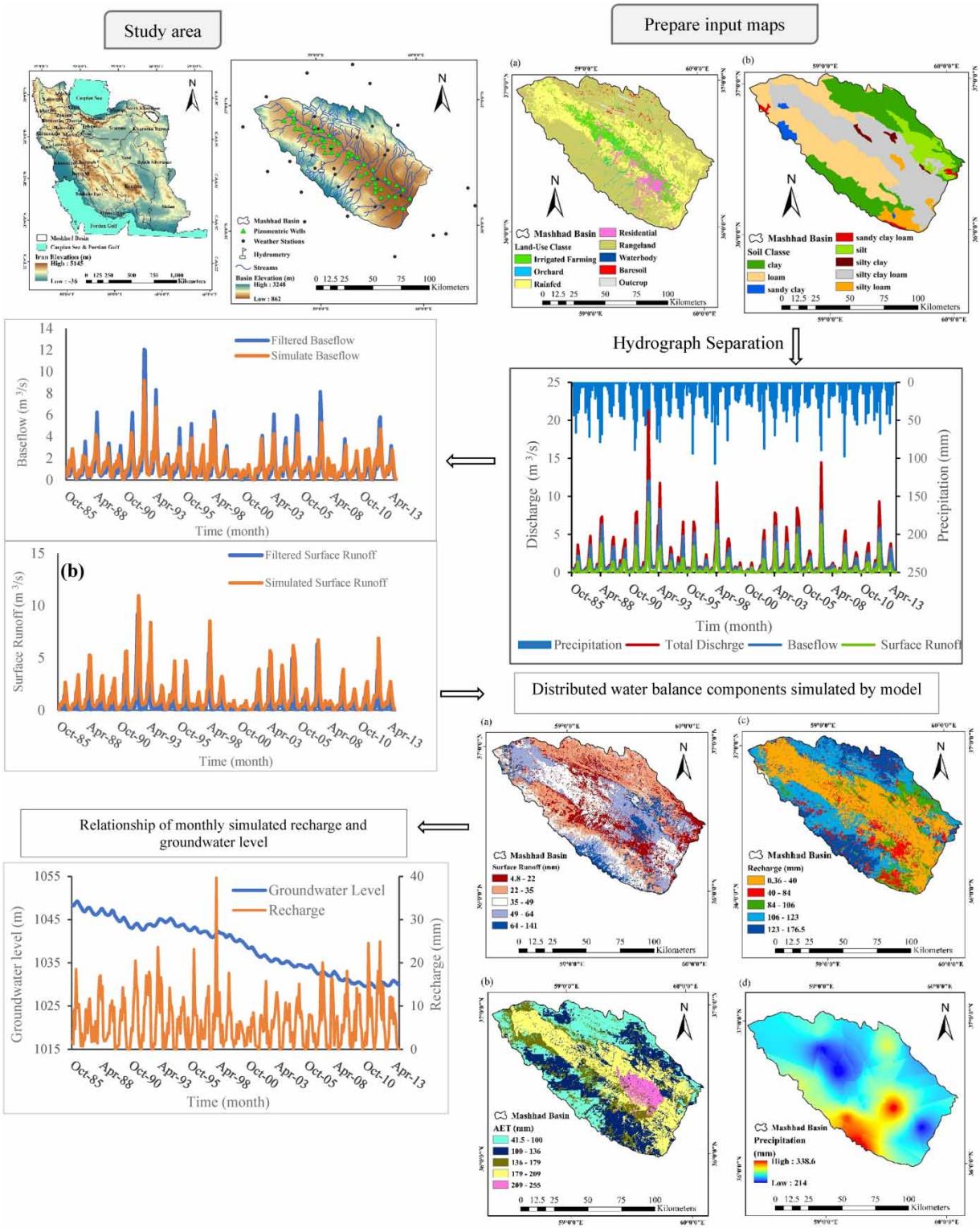

1. INTRODUCTION

Water stands as one of the pivotal limiting factors of agricultural productivity and livestock; moreover, its availability is a critical factor influencing our welfare. Effective water management in arid and semi-arid regions is essential for meeting the diverse water needs of humans, livestock, and ecosystems. Inadequate water resource practices contribute to land degradation and environmental challenges, underscoring the importance of sound water management practices in these regions (Sharma 1998). Estimating the components of water balance becomes imperative for sustainable land and water management, assessing groundwater depletion, evaluating available water, and preventing land degradation. In semi-arid and arid areas, groundwater serves as a vital water source, playing a crucial role in societal development (UN/WWAP 2006; Holger *et al.* 2012; Scanlon *et al.* 2012; Voss *et al.* 2013; Awan & Ismaeel 2014). However, overexploitation of groundwater negatively impacts both its quantity and quality (Scanlon *et al.* 2012). Therefore, assessment of the conditions of groundwater recharge in the semi-arid and arid areas is an important challenge and task to determine the sustainability of the aquifers (Yongxin & Beekman 2003; Crosbie *et al.* 2010).

The recharge of groundwater is the most important factor for determining safe yield (Lerner *et al.* 1990; Xu 2011; Tesfamichael *et al.* 2013). The amounts and locations of the groundwater recharge are also crucial to determine the sustainable use of groundwater resources (Sophocleous & Devlin 2004; Devlin & Sophocleous 2005). Groundwater recharge may be estimated using different methods (e.g., Lerner *et al.* 1990; Simmers 1997; Kinzelbach *et al.* 2002; Xu 2011). Hence, water-budget methods and models can be implemented with different approaches (Xu 2011). Several models such as SWAT (Arnold *et al.* 2000), SVAT (Armbruster & Leibundgut 2001), and DREAM (Manfreda *et al.* 2005), estimate groundwater recharge based on complex hydrological processes. However, in developing countries where hourly and daily climatic data are scarce, their application is limited (Abdollahi *et al.* 2017). The WetSpass model (a spatially distributed hydrological model) assesses the recharge of groundwater on seasonal and annual time scales (Batelaan & De Smedt 2001, 2007). Numerous studies, including those highlighted in this section, have focused on assessing groundwater recharge and surface runoff using the WetSpass model in various countries (Abu-Saleem *et al.* 2010; Arefaine *et al.* 2012; Al-Kuisi & El-Naqa 2013; Tesfamichael *et al.* 2013; Aish 2014). Recently, Salem *et al.* (2019) demonstrated that the mean long-term spatiotemporal monthly rainfall in the Drava basin is divided as runoff (29%), evapotranspiration (27%), and recharge (44%). Ashaolu *et al.* (2020) indicated that 27% of the precipitation in Osun drainage basin, Nigeria, becomes recharge to the aquifer, while the remaining rainfall is lost via evapotranspiration (52%) and surface runoff (21%).

In spite of the water shortage in arid areas of Iran, it is estimated that more than 90% of the freshwater is utilized for agriculture. About 12% of the whole space of Iran (i.e., 19 million hectares) is occupied by agricultural lands. Due to the dependence of most of the country's plains on groundwater resources, especially the Mashhad plain, this area is facing an intense water crisis. The present study concentrates on the Mashhad catchment, Iran, aiming to fill knowledge gaps by meticulously analyzing the spatial and temporal variability of groundwater recharge across different land-use and soil types. The overarching scientific objectives encompass evaluating the WetSpass-M model's capability in estimating water balance component variation, discerning the relative impacts of land-use and climatic data on groundwater level, and assessing mean annual water balance components in diverse land-cover and soil texture combinations. Methodologically, GIS and RS techniques were employed to prepare data, the WetSpass-M hydrological model was applied to assess water balance components (Abdollahi *et al.* 2012), and non-parametric Mann–Kendall tests and Sen's slope estimator were utilized for trend detection. Finally, GIS tools facilitated the integration of water balance component maps with soil and land-use maps. In the context of Iran's arid areas, where over 90% of freshwater supports agriculture and the Mashhad plain faces a severe water crisis, understanding spatial and temporal recharge patterns becomes crucial for sustainable water management. This study contributes detailed information to inform decision-makers, addressing the pressing need for effective water resource management in data-poor regions.

2. MATERIAL AND METHODS

2.1. Description of the study area

The study area is located between east longitude of 58°20′ to 60°8′ and north latitude of 35°58′ to 37°3′ in the North East of Iran (Figure 1). The catchment extent is 9,909 km^2, where the highlands and plains are 6,558 and 3,351 km^2, respectively. The altitude of the mountainous area ranges from 904 to 3,248 m above sea level, and the average slope of the basin is about 9.6%. Most of the precipitation in this area occurs during winter and spring. In terms of climatic conditions, the average long-term

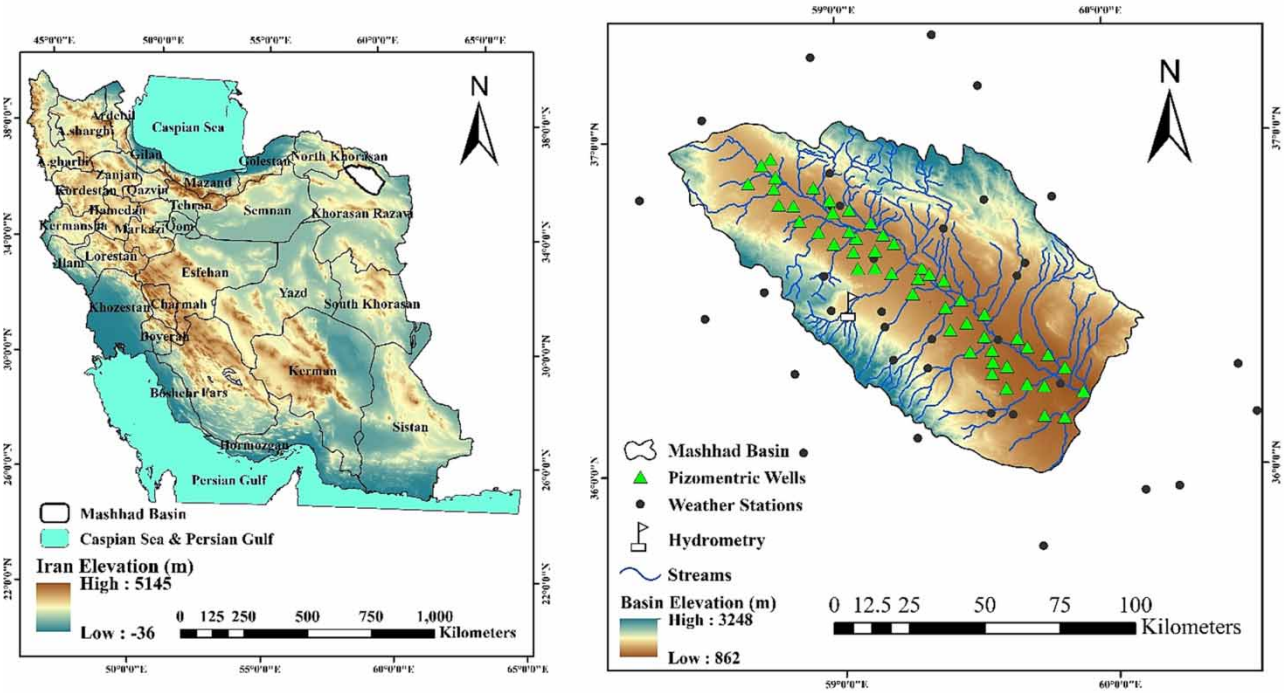

Figure 1 | Geographical location of the Mashhad basin, rivers, used stations (meteorological and hydrometric) and piezometric wells in Khorasan-Razavi Province, Iran.

precipitation in this area is 265 mm/year during the study period (October 1985 to September 2013). Spatially averaged precipitation and pan-evaporation for the study area for the study period are shown in Figure 2. Mashhad Plain is a major center of industry and agriculture in Iran. It is also considered as a crucial center of social–political in the province of Khorasan-Razavi. Because of over-extraction of groundwater, land subsidence occurred in some parts of the study area. Since 1968, new industrial and agricultural activities have been prohibited in the Mashhad catchment (Alem *et al.* 2021). In terms of land use, rangelands and then agricultural lands have occupied the largest area of the study region. Mashhad Plain has been faced with a fast increase rate of population density and economic processes, mainly based on agricultural activities.

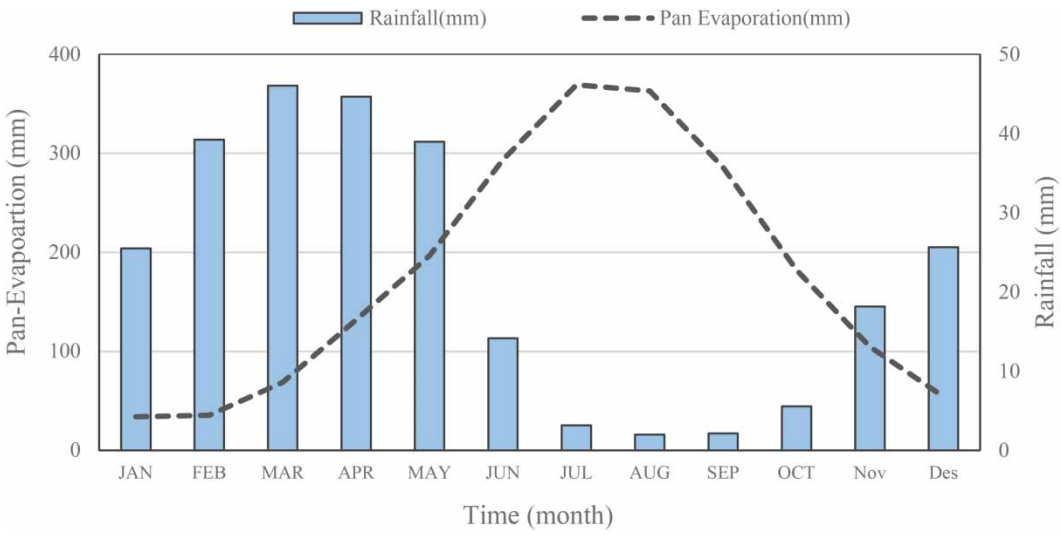

Figure 2 | Long-term spatial average monthly pan-evaporation compared to rainfall for the study period.

Groundwater is considered the principal source of water supply, because of surface water shortage in this area. So, in order to respond to the increasing trend of water requests, groundwater resources have been over extracted during the last years (Bagheri & Hosseini 2011). The total renewable water of Mashhad Plain is 935 Mm^3, while the whole discharge of the aquifer is 1,071 Mm^3 (Dogani *et al.* 2020). The wind direction is mainly from southeast to northwest of the area. Maximum temperature and minimum temperature occur during summer (43 °C) and winter (−23 °C), respectively (Alem *et al.* 2021).

2.2. Overview of the method

The methodological framework employed in this study comprises multiple integrated steps. Initially, remote sensing data and spatial analysis tools were utilized to prepare input data for the WetSpass-M model. Subsequently, this model was applied to ascertain the spatial distribution of water balance components (groundwater recharge, surface runoff, and evapotranspiration). These components were studied in relation to various influencing factors such as groundwater depth, hydrometeorology, topography, land-use type, and soil texture. In the next phase, base-flow analysis was conducted using the Web-based Hydrograph Analysis Tool (WHAT) based on daily river flow data. The identified base-flow was compared with the base-flow simulated by the WetSpass-M model. To evaluate mean annual water balance components across different combinations of soil and land-use data, maps generated by the hydrological model were integrated with soil and land-use maps using spatial analysis tools, specifically the geographic information system. Finally, the Mann–Kendall test and Sen's slope estimator were employed to discern annual trends in groundwater level, precipitation, and simulated water balance component values. The annual slope of statistically significant trends was calculated. A conceptual flowchart illustrating the research steps is presented in Figure 3.

2.2.1. Data preparation for WetSpass-M model

The WetSpass-M model required diverse input data, including distributed land use, monthly leaf area index (LAI), soil textural type, slope map, monthly groundwater depth, and weather data (rainfall, pan-evaporation values, numeral rainy days per month, temperature, and wind speed). The model's grid maps, configured at 631 rows by 467 columns with a cell size of 250 m × 250 m, were established using a digital elevation model (DEM) derived from topography maps at a 1:50,000 scale provided by the Geological Survey and Mineral Exploration of Iran (Figure 1). A corresponding slope map was then generated based on the DEM.

Remote sensing-based and cloud-free Landsat TM (http://earthexplorer.usgs.gov) satellite images were applied to create a land-cover map using ENVI software. In this study, land-use/land-cover (LULC) categorization was conducted by the supervised categorization method with the maximum-likelihood algorithm. The existing land-use classes in the study area were identified through field visits Google Earth images, during which 466 samples (rangeland 128, irrigation farming 76, residential 54, orchard 38, rain-fed farming 115, bare soil 25, outcrop 16, and waterbody 12) were collected to evaluate and verify the accuracy of the prepared land-use maps. The validation findings of provided land-use maps indicated an overall accuracy of 85.6 and 89.7% and a Kappa coefficient of 0.84 and 0.87 for the 1986 and 2013 images, respectively. Eight land-cover classes were identified, which are dominated by the rangeland class (Figure 4(a)). The Mashhad catchment's soil map was prepared according to the maps of land capacity, soil, and soil hydrologic groups generated by the Khorasan-Razavi Agricultural and Natural Resource Center (ANRC) (1996) (Figure 4(b)). Soil texture categories were converted into soil textural types of USGS utilizing the percent of the coarse, medium, and fine particles available in the surface soil and using the saturated hydraulic conductivity of soil hydrologic groups. Eight soil types were determined, i.e., clay, sandy clay, loam, silt, silty loam, sandy clay loam, silty clay, and silty clay loam which are dominated by silty clay loam texture class.

AVHRR and MODIS products were used to obtain the long-term monthly LAI from 1985 to 2013 (available at: ftp://ftp.glcf.umd.edu/glcf/GLASS/LAI/AVHRR), these maps were resampled based on the required pixel size for the study area. Monthly snow cover data from 2000 to 2013 were acquired from MODIS products, while data from 1985 to 2000 were derived through regression analysis of snow, temperature, and rain using Integrated Land and Water Information (ILWIS) software. Groundwater level data (for 50 observation piezometric wells) spanning from October 1985 to September 2013 were sourced from the Regional Water Authority of the Khorasan-Razavi Province. Distributed monthly groundwater depth was determined by subtracting groundwater levels from topographical elevation data. Monthly hydro-climatological variables, such as groundwater depth, precipitation, temperature, pan evaporation, and wind speed, were converted into grid maps using spatial analysis tools. These hydro-climatological data were collected from synoptic and climatology stations

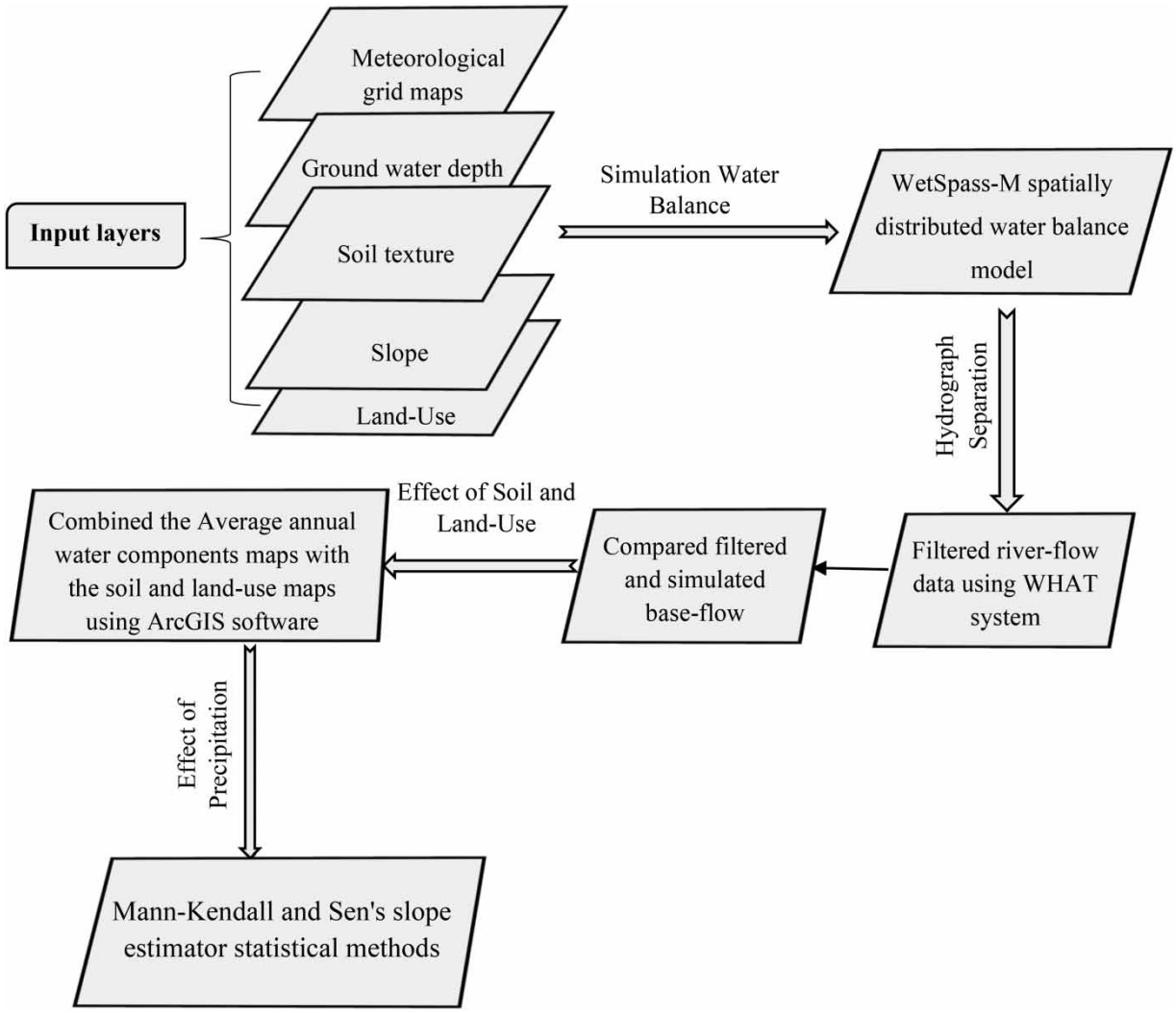

Figure 3 | Conceptual diagram of the different research's steps.

(35 weather stations and one hydrometric station) operated by the Iranian Ministry of Water Resources and Meteorological Organization from October 1985 to September 2013.

2.2.2. WetSpass-M water balance model

The WetSpass-M model, the latest version of the WetSpass model, served as the basis for estimating water balance. This raster-based, quasi-physically distributed monthly hydrological model facilitated the estimation of interception, runoff, evapotranspiration, and recharge for each pixel. The simulation process, initiated with data reading, progressed through monthly water balance components per pixel, encompassing interception, runoff, evapotranspiration, and recharge. The model's flexibility was enhanced through its spatial computational engine, developed by Abdollahi *et al.* (2012, 2017) in IronPython.

Land-cover changes lead to changes in the LAI, consequently estimated interception and evapotranspiration values. The monthly interception is computed by the following equation:

$$I_m = P_m I_R \tag{1}$$

where I_m and P_m are interception and monthly rainfall, respectively (mm/month), and I_R is the ratio of interception.

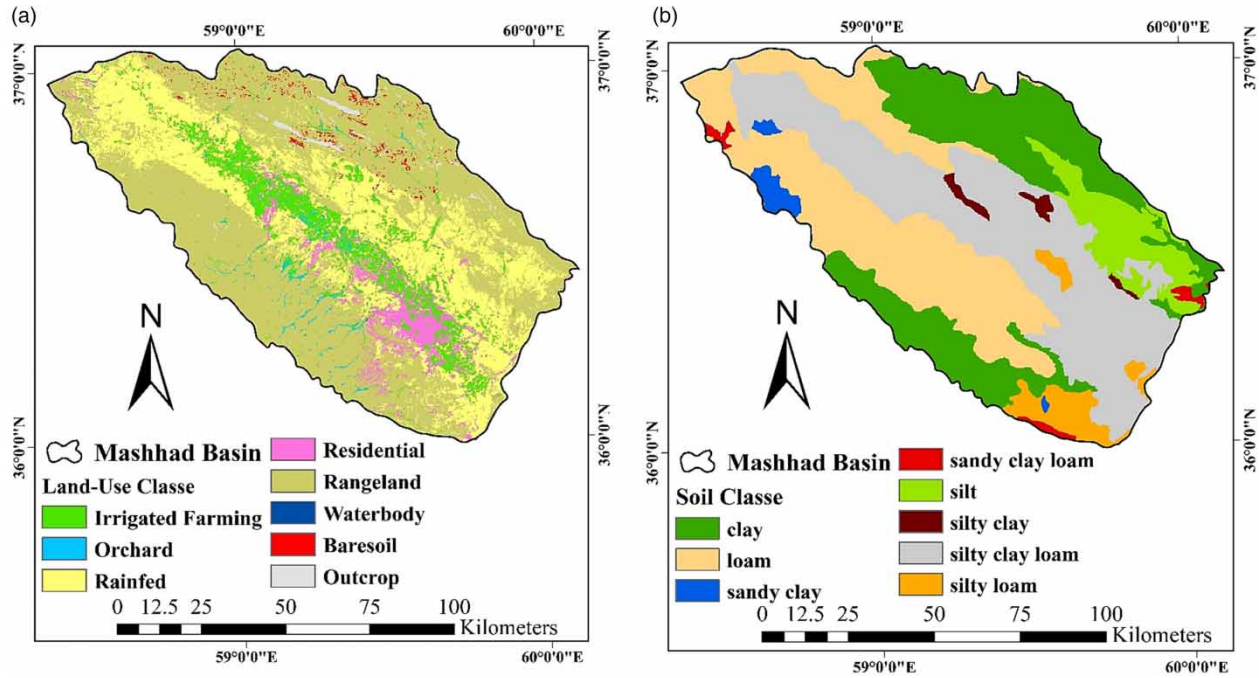

Figure 4 | Spatial variation of land-use types in 1986 (a) and soil types (b) in Mashhad Basin.

Land-use, soil, slope, and rainfall intensity about the soil infiltration capacity affect the surface runoff, which is computed in terms of mm/month utilizing an illustrative technique operated on a monthly basis employing two coefficients (Equation (2)):

$$\mathrm{SR_m} = C_{\mathrm{sr}} C_{\mathrm{h}} (P_{\mathrm{m}} - I_{\mathrm{m}}) \tag{2}$$

$\mathrm{SR_m}$ indicates surface runoff (mm/month), C_{sr} shows the coefficient of surface runoff (implication of the portion of monthly rainfall which participates in surface runoff), C_{h} and I_{m} are a soil moisture-dependent coefficient and the monthly interception, respectively.

Monthly snowmelt simulated based on the linear degree-day relationship between snowmelt and temperature (Equation (3) mm/month):

$$\mathrm{SM} = C_{\mathrm{m}} T_{\mathrm{d}} D_{\mathrm{d}} \tag{3}$$

where SM is monthly snowmelt (mm/month), C_{m} is the coefficient of melt rate (mm/day) or the coefficient of degree-day (°C/day), T_{d} is a daily average temperature (°C), and D_{d} is the number of degree-days per month (Knight *et al.* 2001).

This hydrological model calculates the monthly evapotranspiration for each pixel ($\mathrm{ET_m}$; mm/month) via the following equation:

$$\mathrm{ET_m} = a_{\mathrm{v}} \mathrm{ET_v} + a_{\mathrm{b}} \mathrm{ET_b} + a_0 \mathrm{ET_o} + a_i \mathrm{ET}_i \tag{4}$$

where a_{v}, a_0, a_{b}, and a_i are the area fractions and $\mathrm{ET_V}$, $\mathrm{ET_o}$, $\mathrm{ET_b}$, and ET_i are evapotranspiration for the vegetated region, open water, bare soil, and impervious surface, respectively (Batelaan *et al.* 2003; Abdollahi *et al.* 2017).

Simulating the long-term mean spatial patterns of the groundwater recharge is the principal purpose of utilized hydrological model (Batelaan & De Smedt 2001) which is calculated based on the following equation:

$$R_{\mathrm{m}} = P_{\mathrm{m}} - \mathrm{SR_m} - \mathrm{ET_m} \tag{5}$$

where R_m, P_m, SR_m, and ET_m are groundwater recharge (mm/month), rainfall, surface runoff, and evapotranspiration, respectively.

The monthly base-flow for each cell in the WetSpass-M model is calculated using Equation (6). In this equation, the groundwater recharge in the current month and the storage of the previous month were used (Abdollahi *et al.* 2017):

$$Q_{b(t)} = \beta Q_{b(t-1)} + 0.001\, N_m(1-\beta)\emptyset\, R_m \tag{6}$$

where $Q_{b(t)}$ is the base flow calculated per cell, β shows the storage parameter (0–1), $Q_{b(t-1)}$ is the base flow of the earlier month (m^3/month), N_m stands for the days of each month (≈ 30 days), $\emptyset$ and R_m are the recharge contribution factor to current base flow (m^2/day) and the monthly recharge (mm/month), respectively.

2.2.3. Web-based hydrograph analysis tool

Researchers such as Eckhardt and Gonzales *et al.* have corroborated the effective performance of the WHAT system in assessing water balance evaluation and calibrating hydrological models (Eckhardt 2005; Gonzales *et al.* 2009). In this investigation, the WHAT system was used to partition base flow from river flow (Lim & Engel 2004), employing three separation modules: the one-parameter digital filter technique (Lyne & Hollick 1979; Nathan & McMahon 1990; Arnold & Allen 1999; Arnold *et al.* 2000), the local-minimum method (Lim *et al.* 2005), and the Eckhardt recursive digital filter (Eckhardt 2005). River flow data from the Moshang station, situated on the primary perennial stream, was used for filtration. Iranian Ministry of Water Resources collected and provided these data at daily and monthly intervals covering a period from October 1985 to September 2013. The hydrograph separation tool was applied to daily base data, and monthly base-flow and direct-runoff were computed based on the daily data average over the study period (336-time steps).

Model calibration involved iterative adjustments to input calibration parameters (a, LP, x, α, β, $\varnothing$, and MF, corresponding to interception, surface runoff, runoff delay, evapotranspiration, storage parameter, recharge contribution, and snowmelt, respectively) through trial-and-error process. Sensitivity analysis was conducted on three key parameters (LP, a, and α) as a technique to simplify the model calibration (Abdollahi *et al.* 2017). Calibration and validation of the WetSpass-M model were performed via the comparison of model-simulated data and filtered river flow data using the WHAT method (direct-runoff and base flow).

2.2.4. Mann–Kendall and Sen's slope tests

Mann (1945) and Kendall (1975) developed a rank non-parametric examination named the MK test for statistical testing of the existence of trends. This method is applied to estimate the trend of the hydrologic, climatic, and hydro-meteorological time series (Shahid & Hazarika 2010; Li *et al.* 2018; Tan *et al.* 2019), such as temperature, evapotranspiration, runoff, and rainfall (Sayemuzzaman & Jha 2014; Wang *et al.* 2015). In this test, the alternative (H_a) and null hypotheses (H_o), respectively, correspond to the presence and non-existence of a trend in data time series (Shadmani *et al.* 2012). The MK test statistic S and the Z_{MK} are computed using the following equations:

$$S = \sum_{i-1}^{n-1} \sum_{j=i+1}^{n} \operatorname{sgn}(X_j - X_i) \tag{7}$$

$$\operatorname{sgn}(X_a - X_i) = \begin{cases} +1 & \text{if} \quad (X_a - X_i) > 0 \\ 0 & \text{if} \quad (X_a - X_i) = 0 \\ -1 & \text{if} \quad (X_a - X_i) < 0 \end{cases} \tag{8}$$

$$Z_{MK} = \begin{cases} \dfrac{S-1}{\sqrt{\operatorname{Var}(S)}} & \text{if} \quad S > 0 \\ 0 & \text{if} \quad S = 0 \\ \dfrac{S+1}{\sqrt{\operatorname{Var}(S)}} & \text{if} \quad S < 0 \end{cases} \tag{9}$$

$$\operatorname{Var}(S) = \frac{1}{18}\left[n(n-1)(2n+5) - \sum_{i=1}^{q} t_i(t_i-1)(2t_i+5)\right] \tag{10}$$

where n indicates the numeral of observed data, q shows the numeral of series having at least one replication data, and t represents the number of data that have the same value.

To estimate the true slopes of the significant trends, a simple non-parametric procedure developed by Sen (1986) was applied. The slope estimates via the following equation:

$$Q_i = \frac{X_j - X_g}{j - g} \quad \text{for } i = 1, \ \ldots\ldots, \ N \tag{11}$$

where i represents the number of slopes and the slope estimator of Sen technique is the median of them, X_j and X_g are, respectively, the data values at time j and g $(j > g)$.

3. RESULTS AND DISCUSSION

3.1. Simulation of water balance components

In this section, we present a comprehensive analysis of the hydrological components derived from the WetSpass-M model, shedding light on surface runoff, recharge, interception, and evapotranspiration in the Mashhad catchment. The grid-based maps generated by the WetSpass-M model vividly depict the spatial distribution of water balance components at a pixel level, represented as a coating thickness (in mm) for surface runoff, recharge, interception, and evapotranspiration. The model integrates two crucial coefficients, the actual runoff coefficient (C_{sr}), and soil condition coefficient (C_h), for monthly surface runoff simulation. A detailed examination of the flow hydrograph and its component base-flow and direct-runoff reveals a noteworthy correlation with precipitation, as illustrated in Figure 5. The recursive digital filter method, performed with WHAT, effectively separated base-flow and direct-runoff from total discharge. Sensitivity analysis identified LP as the most influential parameter, with α and a following suit. Altering LP demonstrated a corresponding decrease in runoff and an increase in recharge. This parameter sensitivity order diverges from the previous research by Abdollahi *et al.* (2017), underscoring the local nuances of our study region. Optimum parameters for the WetSpass-M model are detailed in Table 1.

The comparison between base-flow and surface runoff calculated via WHAT and simulated by the WetSpass-M model was used for calibration. The calibration results (for 70% of the total period from October 1985 to March 2005) and validation (for 30% of the whole study period from April 2005 to September 2013), showcased in Figure 6, affirm the model's reliability by

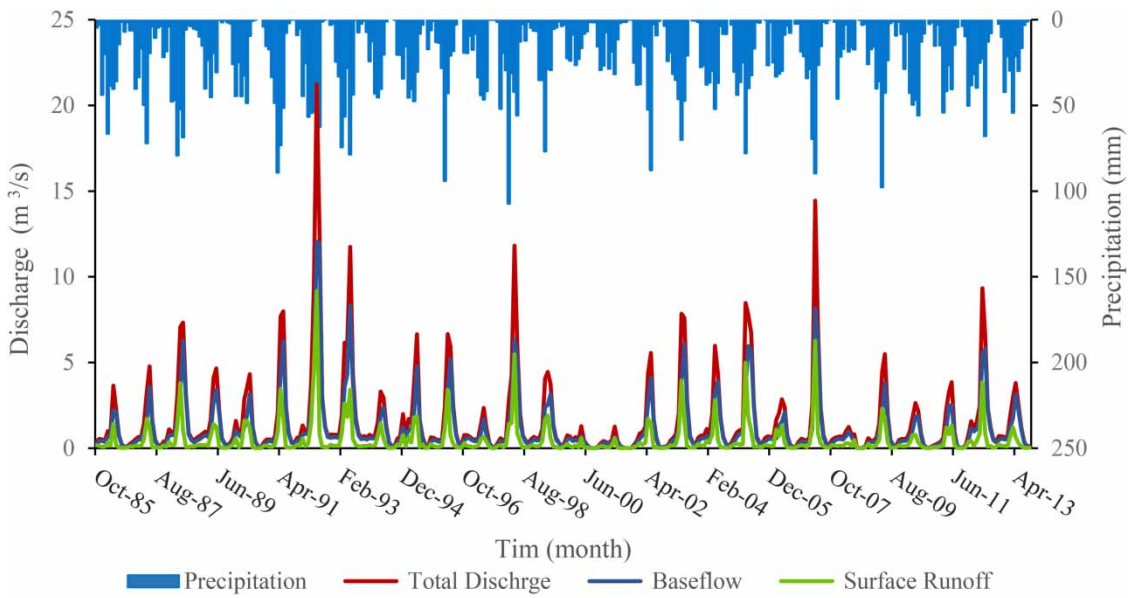

Figure 5 | Monthly precipitation, total discharge, and separated surface runoff and base-flow using WHAT tool.

Table 1 | Optimal values of WetSpass-M model calibration parameters and their typical range

Parameter	Component	Typical range	Optimal value
LP	Surface runoff	0.4–1	0.8
X	Runoff delay	0–1	0.7
A	Interception	0.3–6	3.1
α	Evapotranspiration	0.3–3 <	1.8
β	Base-flow	0–1	0.52

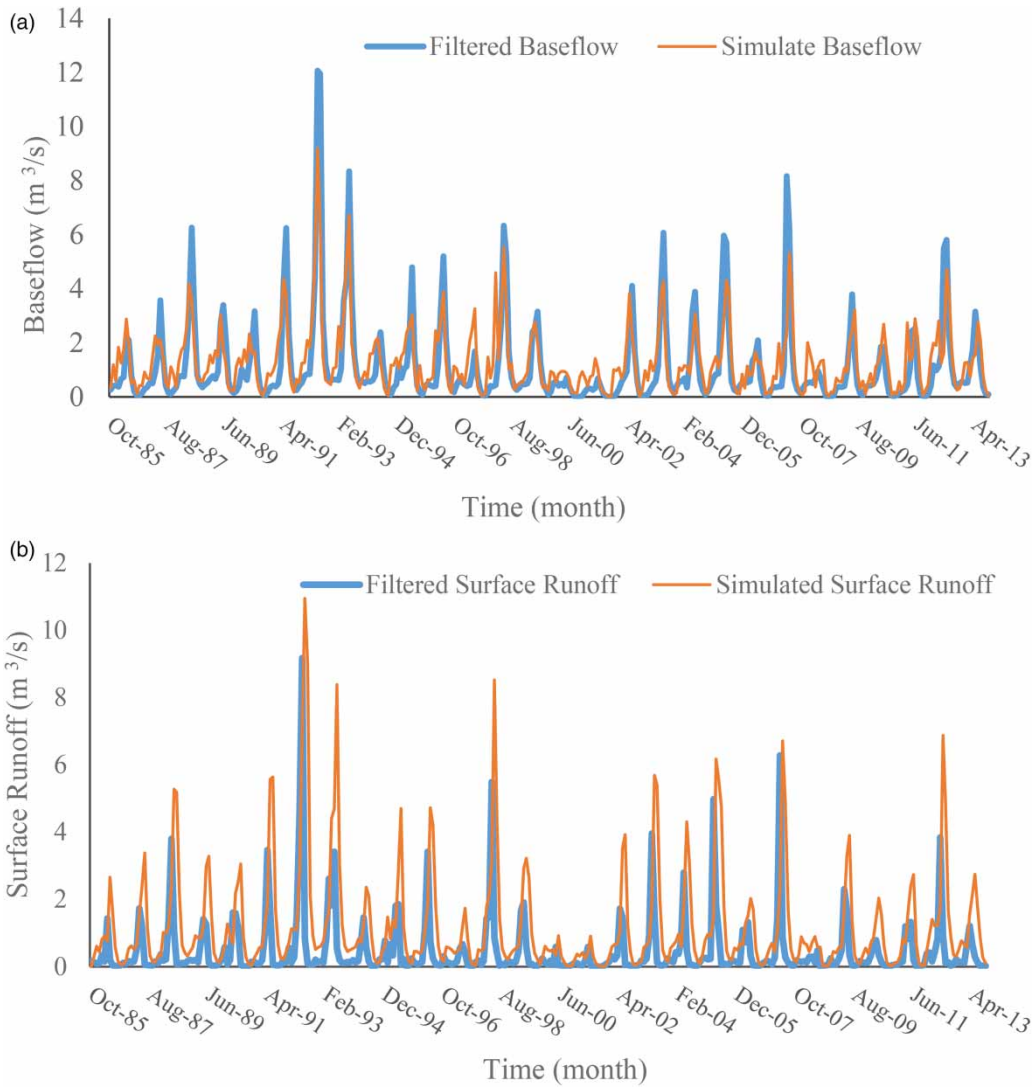

Figure 6 | Comparison of the monthly base-flow and surface runoff filtered from observed discharge versus (a) generated base-flow from simulated recharge and (b) simulated surface runoff.

demonstrating agreement between simulated and filtered data. This consensus is further reinforced through model evaluation presented in Table 2.

Analyzing monthly runoff dynamics in the Mashhad catchment (Table 3) unveils variations from 0 to 41.9 mm/month, with average and standard deviation values of 3.2 and 5 mm/month, respectively. It discovered that about 14% of the total average

Table 2 | Statistical criteria of the WetSpass-M model evaluation

Statistical criteria	Base-flow (m^3/s)	Surface runoff (m^3/s)
R^2	0.76	0.73
NSE	0.74	0.71
RMSE	1.65	0.59

Table 3 | Monthly water balance components of the Mashhad basin during the study period

	Monthly values (mm/month)			
Water balance components	Max	Min	Mean	Std. dev.
Precipitation	107.4	0	22	21.9
Evapotranspiration	63.9	0	12.7	13.4
Recharge	38	0	6.5	5.9
Surface runoff	41.9	0	3.2	4.9
Differences (P–AET–S–R)	22–12.7–3.2–6.5 = − 0.4			

monthly precipitation (22 mm) in the Mashhad basin became surface runoff (3.2 mm) during the study period. This result is higher than compared to the findings of Teklebirhan *et al.* (2012), Al-Kuisi & El-Naqa (2013), and Mathenge *et al.* (2020). For instance, Teklebirhan *et al.* (2012) indicated that as low as 7% of precipitation became surface runoff on the basin located in Northern Ethiopia. On the other hand, this is lower than what was found by Tesfamichael *et al.* (2013), Salem *et al.* (2019), Ashaolu *et al.* (2020) and Zeabraha *et al.* (2020). For instance, in Adigrat area, Northern Ethiopia, Zeabraha *et al.* (2020) observed that about 16% of the annual precipitation became surface runoff. Generally, the comparison with the previous studies highlights both higher and lower percentages, emphasizing the unique hydrological characteristics of our study area.

The estimation of actual evapotranspiration in the Mashhad basin (Table 3), encompassing various land-use classes and soil types, discloses monthly variability (0–63.9 mm) and a substantial contribution (57%) to the water balance. This aligns with earlier research emphasizing the pivotal role of evapotranspiration in watershed water loss (e.g., Tesfamichael *et al.* 2013 Ashaolu *et al.* 2020; Gebru & Tesfahunegn 2020; Mathenge *et al.* 2020; Zeabraha *et al.* 2020). Monthly groundwater recharge, spanning October 1985–September 2013, exhibits variability (0–38 mm), with an average of 6.5 mm (Table 3). Significantly, 29% of the average monthly rainfall contributes to recharge, a proportion exceeding comparable dry regions (e.g., Adelana *et al.* 2006; Teklebirhan *et al.* 2012; Al-Kuisi & El-Naqa 2013; Babama'aji 2013; Tesfamichael *et al.* 2013; Zeabraha *et al.* 2020) but falling below the values reported by Salem *et al.* (2019).

The long-term monthly quota of the water balance elements as a percentage of the rainfall is shown in Table 4. Notably, the lowest percentage of monthly long-term surface runoff occurred in August (1.3%), July (1.4%), September (1.7%), October

Table 4 | Percentage of long-term average monthly water balance components simulated by WetSpass-M model compared to total monthly precipitation during the study period (percent of precipitation)

Month	Jan	Feb	Mar	Apr	May	Jun	Jul	Aug	Sep	Oct	Nov	Dec
Precipitation (mm)	25.5	39.2	46	44.6	39	14.2	3.2	2	2.1	5.5	18.1	25.6
Evapotranspiration (%)	31.9	33.3	46.6	50.9	51.1	51.6	61.4	60.9	56.9	49.1	46.4	41.4
Recharge (%)	26.9	26.1	20.4	27.2	35.7	42.8	36.2	35.9	39.4	44.3	32.2	25.4
Interception (%)	22.8	20.4	18.3	11.3	5.1	1.8	1	2	1.9	4.2	12.8	18.8
Surface runoff (%)	20.9	22.2	17.3	12.7	9.7	4.4	1.4	1.3	1.7	3.1	11	16.5
Balance error	−2.5	−2	−2.6	−2.1	−1.6	−0.6	0	−0.1	0.1	−0.7	−2.4	−2.1

(3.1%), and June (4.4%). During these months, the vegetation cover in the area is more than in other months. Change in monthly surface runoff can also be related to the unequal temporal distribution of precipitation in different months (Figure 7). For all monthly water balance components except for the months of June to October, the highest percentage of precipitation is associated with evapotranspiration (Table 4). Accordingly, higher amounts of evapotranspiration are discovered during the months which receive more precipitation. Most of the evapotranspiration occurs during the month of November (235.1 mm) to May (557.5 mm) (Figure 7). The results of this study are consistent with the findings of the studies by Arefaine *et al.* (2012), Al-Kuisi & El-Naqa (2013), and Tesfamichael *et al.* (2013). According to the results of Table 4, the highest percentage of recharge to the aquifer occurred in the months of June to October, when minimum runoff and evapotranspiration were noted.

3.2. Water balance components in different combined land use and soil

The long-term average annual runoff map (Figure 8(a)) is computed using the monthly simulated maps per year. According to the results, the maximum values are observed in the center (close to the Mashhad Mega City), northwest, and southwest regions of the catchment which is correlated with the higher average annual precipitation (Figure 8(d)). Table 5 provides insight into surface runoff disparities across soil and land-use types, emphasizing the influence of clay soils on increased runoff. Accordingly, the highest value of surface runoff in the study area occurred in the silty loam and clay soils with rain-fed farming, this is because of the low permeability of clay soil which increases the runoff. The finding is the same as the previous observations by Babama'aji (2013) in the Lake Chad catchment, Salem *et al.* (2019) in Drava Basin in Hungary and Ashaolu *et al.* (2020) in Nigeria, West Africa, On the other hand, the lowest values of surface runoff occur in silty clay, sandy clay, and silty clay loam soils with rangeland. These results are at variant with what Al-Kuisi & El-Naqa (2013) reported in the arid Jafr catchment, Jordan, where relatively high surface runoff was observed in silty clay soil. It is also inconsistent with the findings of Tesfamichael *et al.* (2013) who stated that the highest runoff occurs on sandy clay soils. The findings of various combinations of soil and land-use types clearly indicated that the soil influenced more on the spatial distribution of runoff than land use, which is in good agreement with what was found in earlier researches (Teklebirhan *et al.* 2012; Al-Kuisi & El-Naqa 2013; Babama'aji 2013; Tesfamichael *et al.* 2013; Ashaolu *et al.* 2020). Overall, these findings reinforce the dominance of soil characteristics in runoff patterns.

The average annual evapotranspiration for 28 years was calculated by adding monthly evapotranspiration maps (Figure 8(b)) and is higher in regions with higher vegetation cover and agricultural land. Table 6 reveals the variability of evapotranspiration among the various combinations of soil and land use. Silty loam and silty clay loam soils exhibit the highest evapotranspiration, while the lowest value was obtained for clay soil. The irrigation farming, rain-fed farming, and orchard land uses display the greatest amounts of evapotranspiration, meanwhile, the lowest values are revealed in rangeland and residential land-use classes. Tesfamichael *et al.* (2013) reported that evapotranspiration in their case study was more affected

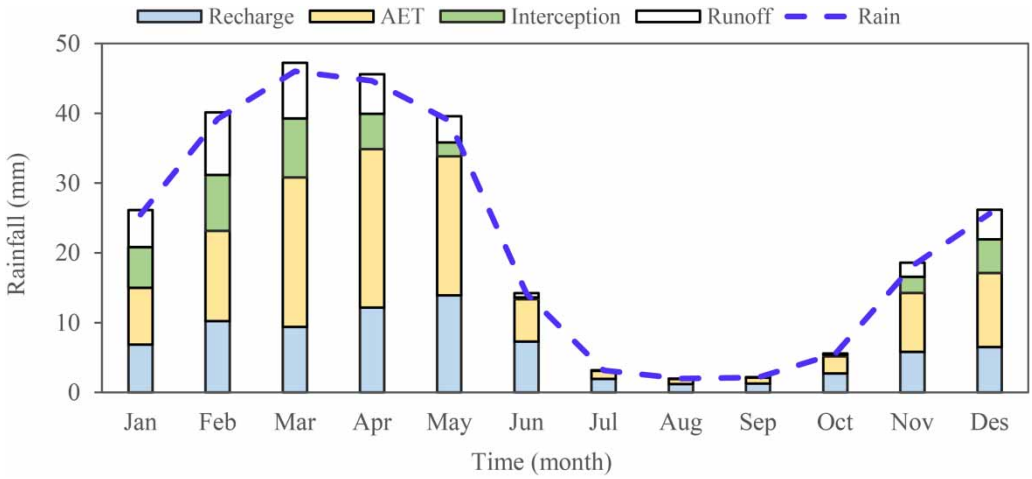

Figure 7 | Temporal variation of long-term average monthly water balance components and their proportion to precipitation during the study period.

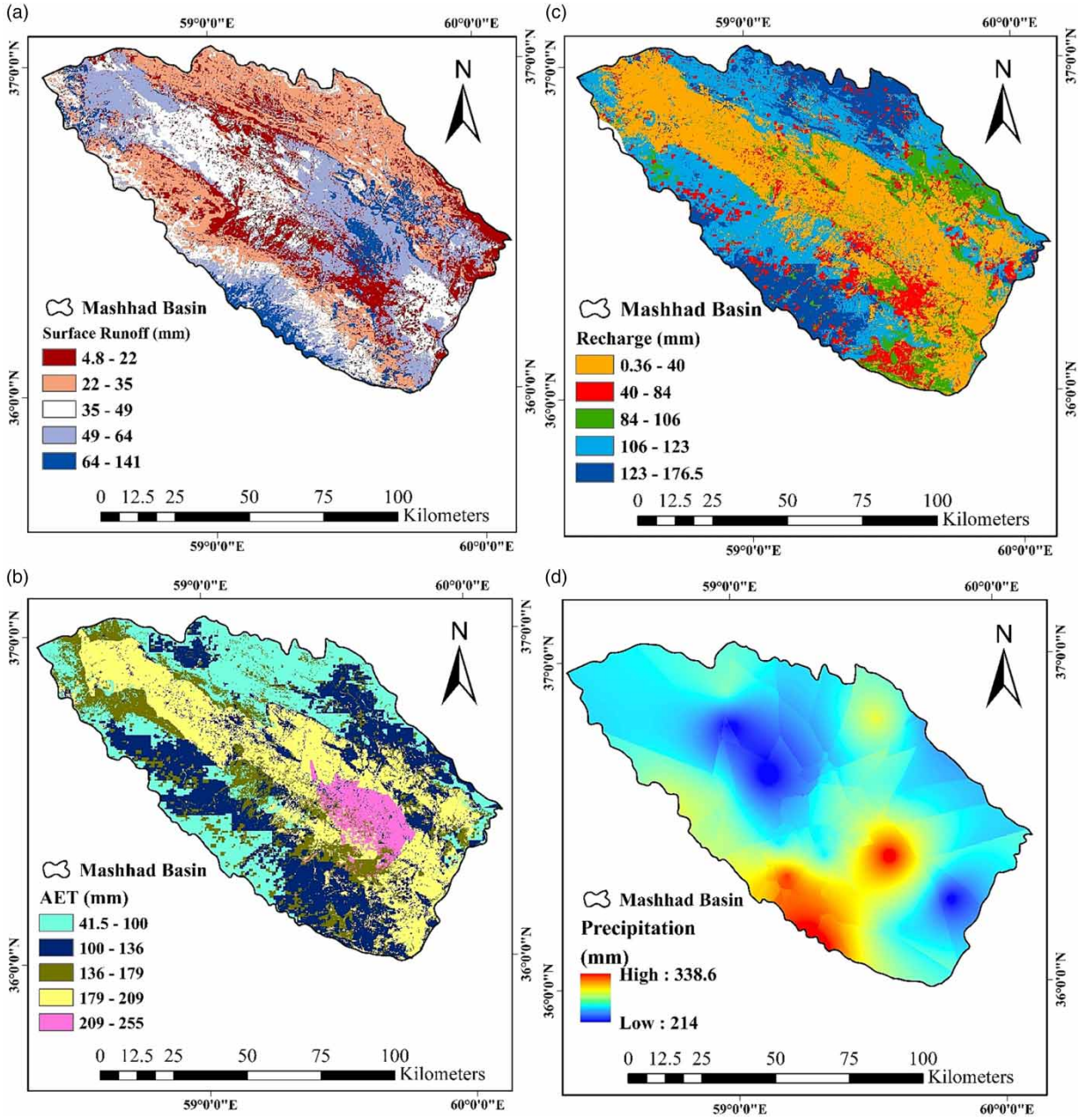

Figure 8 | Spatial maps of water balance components simulated by WetSpass-M model and precipitation: (a) average yearly runoff (mm), (b) average yearly AET (mm), (c) average yearly recharge (mm), and (d) average yearly precipitation (mm).

by land-use class than soil texture and the same result was found in our study area which shows that evapotranspiration is more changeable within land cover than soil texture (Table 6).

The annual recharge maps were created based on monthly simulated recharge maps (Figure 8(c)). The lowest values of groundwater recharge were observed in the flat parts of the catchment, probably due to a mixture of desirable circumstances such as more surface runoff and more evapotranspiration and more vegetation cover. Soil textural types and land-cover classes had a significant impact on groundwater recharge. The average annual groundwater recharge amounts for various mixtures of soil and land-use categories are indicated in Table 7. It seems that loamy and sandy clay soils with rangeland have the highest amounts of groundwater recharge, basically due to the high permeability of these soils. Agricultural lands with the soil classes of silty loam, silty clay, and sandy clay loam soils have the lowest values, which is clearly due to the

Table 5 | Mean annual surface runoff simulated by WetSpass-M model for combinations of land-use and soil texture (mm)

	Clay	Loam	Sandy clay	Sandy clay loam	Silt	Silty clay	Silty clay loam	Silty loam	Mean	Std.dev.
Irrigation farming	62	59	67	75	64	65	64	82	67	7
Residential	48	33	33	33	25	28	27	44	34	8
Rangeland	35	26	23	35	25	22	23	37	28	6
Rain-fed farming	84	63	68	77	68	59	60	92	71	12
Bare soil	41	42	[a]	[a]	51	41	47	[a]	44	4
Orchard	63	55	67	55	48	[a]	38	72	57	12
Mean	55.5	46	52	55	47	43	43	65		
Std. dev.	18	15	22	21	19	19	17	24		

[a]There is no region with this specific combination of soil and land-use in the study area.

Table 6 | Mean annual evapotranspiration simulated by WetSpass-M model for combinations of land-use and soil texture (mm)

	Clay	Loam	Sandy clay	Sandy clay loam	Silt	Silty clay	Silty clay loam	Silty loam	Mean	Std.dev.
Irrigation farming	179	187.5	195	196	194	200	213	220	198	13
Residential	124	134	99	121	130	138	151	142	130	16
Rangeland	118	121	114	122	128	129	145	143	127	11
Rain-fed farming	75	187	191	196	196	199	214	216	184	45
Bare soil	157	163	[a]	[a]	187	168	186	[a]	172	14
Orchard	181	193	172	177	170	[a]	192	178	180	9
Mean	139	164	154	162	167	167	183	179.8		
Std. dev.	41	30	45	38	31	33	30	38		

[a]There is no region with this specific combination of soil and land-use in the study area.

Table 7 | Mean annual recharge simulated by WetSpass-M model for combinations of land-use and soil texture (mm)

	Clay	Loam	Sandy clay	Sandy clay loam	Silt	Silty clay	Silty clay loam	Silty loam	Mean	St.dev.
Irrigation farming	27	20	6	2.5	5	2	4	2	9.4	10
Residential	39	45	52	49	44	36	36	32	41	7
Rangeland	105	108	114	94	90	77	85	80	94	14
Rain-fed farming	27	20	8	3	5.5	2.5	4	2	10.6	10
Bare soil	56	48	[a]	[a]	27	27	25	[a]	36.6	14
Orchard	46	37	19	16	24	[a]	19	12	24.7	12
Mean	56	49	43	40.5	38	35.5	29	26		
St. dev.	29	33	45	41	32	31	30	33		

[a]There is no region with this specific combination of soil and land-use in the study area.

high transpiration, evaporation losses, high temperature, and low precipitation in these flat regions. The higher standard deviation amounts of the recharge for various soil textures (Table 7) show that soil texture has more impact on recharge than land-use classes. This underscores the predominant impact of soil characteristics on recharge, consistent with what was reported by Babama'aji (2013), while is inconsistent with the findings of Ashaolu *et al.* (2020) who indicated that recharge in Nigeria was more affected by land-use type.

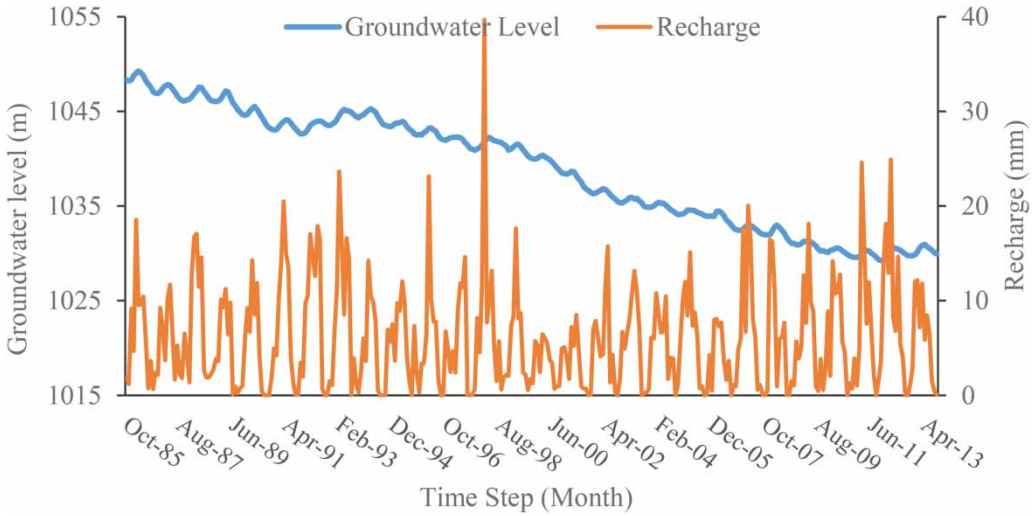

Figure 9 | Relationship between monthly groundwater recharge and groundwater level from October 1985 to September 2013.

3.3. Trend detection

Figure 9 shows the relationship between monthly groundwater recharge simulated using WetSpass-M model and the observed groundwater level from the aquifer's hydrograph. A notable annual decline of about 0.66 m per year is observed, with the statistical significance attributed solely to groundwater level trends (Table 8). Analysis trends in annual groundwater level, annual precipitation, and simulated water balance components in the Mashhad basin indicate that only the groundwater level has a statistically significant subtractive trend. This decline, coupled with land-use changes (Table 9), implies over extraction due to human activities. Accordingly, irrigation farming, residential (including industrial), orchard, and bare soil area were increased by 45.3% (393 km^2), 63% (321.4 km^2), 196% (152.2 km^2), and 166% (115.9 km^2), respectively. Therefore, it can be concluded that the groundwater level has probably decreased due to the over extraction of groundwater for irrigation, drinking, and industrial purposes during the study period. Our hydrological analysis, facilitated by the WetSpass-M model, unveils intricate water balance dynamics in the Mashhad catchment. The nuanced interplay of parameters, validated by comprehensive comparisons, emphasizes the model's reliability. The unique hydrological characteristics observed underscore the importance of local conditions in shaping water balance outcomes.

4. CONCLUSIONS

In this study, we employed the WetSpass-M model, a raster-based quasi-physically distributed monthly hydrological model, to comprehensively assess the monthly water balance components in the Mashhad catchment. Utilizing a combination of the WetSpass-M model, WHAT (WHAT), and non-parametric trend analysis tests, we evaluated various hydrological aspects and identified trends in the data. Spatial analysis techniques were integral in preparing the extensive input data required

Table 8 | Statistics of the annual trends of simulated water components, groundwater level, and precipitation

	Mann–Kendall trend		Sen's slope estimates	
Time series	**Test *Z***	***Q***	***Q* min 95%**	***Q* max 95%**
Simulated recharge (mm/year)	−0.65	−0.21	−1.28	0.641
Groundwater level (m/year)	−7.05[a]	−0.73	−0.792	−0.888
Simulated runoff (mm/year)	−0.30	−0.097	−0.847	0.744
Evapotranspiration (mm/year)	−1.17	−1.05	−3.290	0.918
Precipitation (mm/year)	−0.81	−1.45	−5.067	1.95

[a]Significant in 5% level.

Table 9 | Percentage of land-use change from 1986 to 2013

Land-use class	1986 (km^2)	2013 (km^2)	Changes (km^2)	Changes ≍ (%)
Rangeland	5,331.52	4,504.67	−826.85	−15.5
Irrigation farming	867.46	1,260.49	+393.03	+45.3
Residential and industrial	509.85	831.26	+321.41	+63
Orchard	77.65	229.87	+152.21	+196
Bare soil	69.67	185.58	+115.92	+166.4
Rain-fed farming	2,983.06	2,824.52	−158.54	−5.3

−Indicates a decrease, +indicates an increase.

for the model. Our results highlight that the average monthly evapotranspiration, constituting 57% (12.7 mm) of the monthly precipitation (22 mm), is primarily influenced by precipitation and vegetation cover. Notably, long-term average monthly evapotranspiration increased with rising monthly precipitation, with rain-fed and irrigation farming lands, along with silty loam soils, exhibiting the highest evapotranspiration. Examining the monthly runoff, we observed variations ranging from 0 to 41.9 mm, with an average of 3.2 mm, representing 14% of the monthly precipitation. The highest surface runoff occurred in irrigation farming areas on silty loam and clay soils. Monthly recharge of the Mashhad catchment ranged from 0 to 38 mm, averaging 6.5 mm per month, constituting 29% of the monthly precipitation, with the highest amount occurring in sandy clay soils with rangeland.

Spatially, the largest surface runoff amounts were observed in the southwest and central regions of the catchment, correlating with higher rainfall. Additionally, areas with low elevation exhibited higher evapotranspiration and lower groundwater recharge compared to the high-altitude regions. Combining simulated maps using the WetSpass-M model with soil and land-use maps revealed that evapotranspiration varies more within land-use classes compared to soil texture types, while soil texture had a greater impact on recharge and surface runoff compared to land use in the Mashhad Basin. Only groundwater depth showed a statistically significant declining trend post the 1990s, while precipitation and simulated water components trends were not statistically significant. The increase in irrigation farming area, residential area, and orchard land cover from 1986 to 2013 suggests a potential influence on the declining groundwater levels in the Mashhad mega city. The significant decline in groundwater level at a rate of 0.66 mm per year, coupled with changes in land cover, suggests that human activities are leading to over extraction.

In summary, the integrated approach of the WetSpass-M model, coupled with comprehensive spatial analysis and trend assessments, provides valuable insights into the intricate hydrological processes of the Mashhad catchment. Our study contributes to a deeper understanding of water balance dynamics, aiding in the formulation of informed water resource management strategies amidst evolving land-use patterns and climate variations. Our study has provided valuable insights into the recharge dynamics of the study area. The observed trend changes in recharge are subject to certain limiting conditions, including the spatiotemporal variability of precipitation, the hydrogeological characteristics of the study area, and the impact of human activities on groundwater resources. Therefore, the results may not be applicable to all regions or under all circumstances. Nonetheless, our findings highlight the critical importance of sustainable water management practices to mitigate the impact of human activities on groundwater resources. Further research is needed to better understand the complex interactions between climate, land use, and groundwater resources and to develop effective strategies for sustainable water management in arid and semi-arid regions.

ACKNOWLEDGEMENTS

The authors appreciate the Iranian Meteorological Organization (IRIMO) and Iran Water Resources Company for providing the observational daily hydro-meteorological and hydrogeological data of the study area. We also are grateful to the Department of Civil, Environmental, Architectural Engineering and Mathematics, University of Brescia, Italy for providing scientific support for this research.

DATA AVAILABILITY STATEMENT

All relevant data are included in the paper or its Supplementary Information.

CONFLICT OF INTEREST

The authors declare there is no conflict.

REFERENCES

Abdollahi, K., Bashir, I. & Batelaan, O. 2012 *WetSpass Graphical User Interface*. Version 31-05-2012. Vrije University Brussel, Department of Hydrology and Hydraulic Engineering, Brussels, Belgium.

Abdollahi, K., Bashir, I., Verbeiren, B., Harouna, M. R., Griensven, A. V., Husmans, M. & Batelaan, O. 2017 A distributed monthly water balance model: Formulation and application on Black Volta Basin. *Environmental Earth Science* **76** (5), 198. https://doi.org/10.1007/s12665-017-6512-1.

Abu-Saleem, A., Al-Zubi, Y., Rimawi, O., Al-Zubi, J. & Alouran, N. 2010 Estimation of water balance components in the Hasa basin with GIS based WetSpass model. *Journal of Agronomy* **9** (3), 119–125. doi: 10.3923/ja.2010.119.125.

Adelana, S. M. A., Olasheinde, P. I. & Vrbka, P. 2006 A quantitative estimation of groundwater recharge in part of the Sokoto Basin, Nigeria. *Journal of Environmental Hydrology* **14** (5), 1–16.

Aish, A. M. 2014 Estimation of water balance components in the Gaza Strip with GIS based WetSpass model. *Civil and Environmental Research* **6** (11), 77–84. ISSN 2224-5790 (Paper). https://www.iiste.org/Journals/index.php/CER/article/view/17076

Alem, H., Esmaeilzadeh Soudejani, A. & Fallahi, M. 2021 Estimate the amount of ground water recharge in hard formations, case study: Mashhad, Iran. *Applied Water Science* **11**, 6. https://doi.org/10.1007/s13201-020-01317-w.

Al-Kuisi, M. & El-Naqa, A. 2013 GIS based spatial groundwater recharge estimation in the Jafr Basin, Jordan – application of WetSpass models for arid regions. *Revista Mexican de Ciencias Geologicas* **30**, 96–109.

Arefaine, T., Nedaw, D. & Tesfamicheal, G. 2012 Groundwater recharge, evapotranspiration and surface runoff estimation using WetSpass modeling method in Illala catchment, Northern Ethiopia. *Momona Ethiopian Journal of Science (MEJS)* **4**, 96–110. doi: 10.4314/mejs.v4i2.80119.

Armbruster, V. & Leibundgut, C. 2001 Determination of spatially and temporally highly detailed groundwater recharge in porous aquifers by a SVAT model. *Physics and Chemistry of the Earth Part B* **26** (7–8), 607–611. https://doi.org/10.1016/S1464-1909(01)00056-9.

Arnold, J. G. & Allen, P. M. 1999 Validation of automated methods for estimating baseflow and groundwater recharge from stream records. *Journal of American Water Resources Association* **35**, 411–424. https://doi.org/10.1111/j.1752-1688.1999.tb03599.x.

Arnold, J. G., Muttiah, R. S., Srinivasan, R. & Allen, P. M. 2000 Regional estimation of baseflow and groundwater recharge in the upper Mississippi River basin. *Journal of Hydrology* **227**, 21–40. https://doi.org/10.1016/S0022-1694(99)00139-0.

Ashaolu, E. D., Olorunfemi, J. F., Ifabiyi, I. P., Abdollahi, K. & Batelan, O. 2020 Spatial and temporal recharge estimation of the basement complex in Nigeria, West Africa. *Journal of Hydrology: Regional Studies* **27.** https://doi.org/10.1016/j.ejrh.2019.100658

Awan, U. K. & Ismaeel, A. 2014 A new technique to map groundwater recharge in irrigated areas using a SWAT model under changing climate. *Journal of Hydrology* **519**, 1368–1382. http://dx.doi.org/10.1016/j.jhydrol.2014.08.049.

Babama'aji, R. A. 2013 *Impacts of Precipitation, Land Use Land Cover and Soil Type on the Water Balance of Lake Chad Basin*. PhD Thesis. University of Missouri-Kansas City.

Bagheri, A. & Hosseini, S. A. 2011 A system dynamics approach to assess water resources development scheme in the Mashhad plain, Iran, versus sustainability. In *ASCE Conference*. https://www.researchgate.net/publication/230851817.

Batelan, O. & De Smedt, F. 2001 *WetSpass: A Flexible, GIS Based, Distributed Recharge Methodology for Regional Groundwater Modelling*, Vol. 269. IAHS Publication, Maastricht, The Netherlands, pp. 11–18.

Batelaan, O. & De Smedt, F. 2007 GIS-based recharge estimation by coupling surface-subsurface water balances. *Journal of Hydrology* **337** (3), 337–355. https://doi.org/10.1016/j.jhydrol.2007.02.001.

Batelaan, O., De Smedt, F. & Triest, L. 2003 Regional groundwater discharge: Phreatophyte mapping, groundwater modelling and impact analysis of land-use change. *Journal of Hydrology* **275** (1–2), 86–108. https://doi.org/10.1016/S0022-1694(03)00018-0.

Crosbie, R., Jolly, L., Leaney, F., Petheram, C. & Wohling, D. 2010 *Review of Australian Groundwater Recharge Studies CSIRO: Water for a Healthy Country National Research Flagship Report Series ISSN: 1835-095X*.

Delvin, J. F. & Sophocleous, M. 2005 The persistence of the water budget myth and its relationship to sustainability. *Hydrogeology Journal* **13**, 549–554. https://doi.org/10.1007/s10040-004-0354-0.

Dogani, A., Dourandish, A. & Ghorbani, M. 2020 Ranking of resilience indicators of Mashhad plain to groundwater resources reduction by Bayesian best-worst method. *Iranian Journal of Water and Irrigation Management* **10** (2), 301–316. https://jwim.ut.ac.ir/article_78121.html?lang=en

Eckhardt, K. 2005 How to construct recursive digital filters for base flow separation. *Hydrological Processes* **19** (2), 507–515. https://doi.org/10.1002/hyp.5675.

Gebru, T. A. & Tesfahunegn, G. B. 2020 GIS based water balance components estimation in Northern Ethiopia catchment. *Soil Tillage Research* **197**, 104514. https://doi.org/10.1016/j.still.2019.104514.

Gonzales, A., Nonner, J., Heijkers, J. & Uhlenbrook, S. 2009 Comparison of different base flow separation methods in a lowland catchment. *Hydrology and Earth System Sciences* **13** (11), 2055–2068. https://doi.org/10.5194/hess-13-2055-2009.

Holger, T., Martin-Bordes, J. L. & Jason, J. G. 2012 Climate change effects on groundwater resources. *International Association of Hydrogeologists* **414**, ISBN 9780367576820.

Kendall, M. G. 1975 Rank Correlation Methods, 4th edn. Charles Griffin, London.

Khorasan-Razavi Agricultural and Natural Resource Center (ANRC) 1996 *A Report of Soil and Water Resources Management in the Mashhad Plain (in Persian)*.

Kinzelbach, W., Aeschbach, W., Alberich, C., Goni, I. B., Beyerle, U., Brunner, P., Chiang, W. H., Rueedi, J. & Zollmann, K. 2002 *A Survey of Methods for Groundwater Recharge in Arid and Semi-Arid Regions. Early Warning and Assessment Report Series, UNEP/DEWA/RS. 02-2*. United Nations Environment Programme, Nairobi. http://wedocs.unep.org/handle/20.500.11822/8195

Knight, C. G., Chang, H., Staneva, M. P. & Kostov, D. 2001 A simplified basin model for simulating runoff: The Struma River GIS. *Professional Geographer* **53** (4), 533–545. https://doi.org/10.1111/0033-0124.00303.

Lerner, D. N., Issar, A. S. & Simmers, I. 1990 Groundwater recharge: A guide to understanding and estimating natural recharge. In: *IAH International Contributions to Hydrogeology*, Vol. 8. (Hendrickx, I. M. H., ed.) Verlag, Heinz Heise, Hanover. 345 p. ISBN 3-922705-91-X.

Li, C., Filho, W. L., Wang, j., Fudjimdjum, H., Fedork, M., Hu, R., Yin, S., Bao Yu, S. & Hunt, J. 2018 An analysis of precipitation extremes in the inner Mongolian plateau: Spatial-temporal patterns, causes, and implications. *Atmosphere* **9**, 322. https://doi.org/10.3390/atmos9080322.

Lim, K. J. & Engel, B. A. 2004 *WHAT: Web-Based Hydrograph Analysis Tool*. Available from: http://pasture.ecn.purdue.edu/~what (accessed September 2005).

Lim, K. J., Engel, B. A., Tang, Z., Choi, J., Kim, K. S., Muthukrishnan, S. & Tripathy, D. 2005 Automated web GIS based hydrograph analysis tool, WHAT. *Journal of American Water Resource Association* **41** (6), 1407–1416. https://doi.org/10.1111/j.1752-1688.2005.tb03808.x.

Lyne, V. D. & Hollick, M. 1979 Stochastic time-variable rainfall-runoff modeling. In *Hydrology and Water Resource Symposium Institution of Engineers Australia*, Perth, Australia, pp. 89–93.

Manfreda, S., Fiorentino, M. & Iacobellis, V. 2005 DREAM: A distributed model for runoff, evapotranspiration, and antecedent soil moisture simulation. *Advances in Geosciences* **2**, 31–39. https://doi.org/10.5194/adgeo-2-31-2005.

Mann, H. B. 1945 Non-parametric tests against trend. *Econmetrica* **13**, 245–259. http://dx.doi.org/10.2307/1907187.

Mathenge, M. W., Gathuru, G. M. & Kitur, E. L. 2020 Spatial-temporal variation of groundwater recharge from precipitation in the Stony Athi sub-catchment, Kenya. *International Journal of Environmental Sciences* **3** (1), 21–41.

Nathan, R. J. & McMahon, T. A. 1990 Evaluation of automated techniques for baseflow and recession analysis. *Water Resource Research* **26** (7), 1465–1473. https://doi.org/10.1029/WR026i007p01465.

Salem, A., Dezső, J. & Mustafa, E.-R. 2019 Assessment of groundwater recharge, evaporation, and runoff in the Drava Basin in Hungary with the WetSpass model. *Hydrology* **6** (1), 23. https://doi.org/10.3390/hydrology6010023.

Sayemuzzaman, M. & Jha, M. K. 2014 Seasonal and annual precipitation time series trend analysis in North Carolina, United States. *Atmospheric Research* **137**, 183–194. https://doi.org/10.1016/j.atmosres.2013.10.012.

Scanlon, B. R., Faunt, C. C., Longuevergnec, L., Reedya, R. C., Alley, W. M., McGuired, V. L. & McMahone, P. B. 2012 Groundwater depletion and sustainability of irrigation in the US High Plains and Central Valley. *PNAS* **109** (24), 9320–9325. doi: 10.1073/pnas.1200311109.

Sen, P. K. 1986 Estimates of regression coefficient based on Kendall's tau. *Journal of American Statistical Association* **63**, 1379–1389. https://doi.org/10.1080/01621459.1968.10480934.

Shadmani, M., Marofi, S. & Roknian, M. 2012 Trend analysis in reference evapotranspiration using Mann-Kendall and Spearman's Rho tests in arid regions of Iran. *Water Recourse Management* **26** (1), 211–224. https://doi.org/10.1007/s11269-011-9913-z.

Shahid, S. & Hazarika, M. K. 2010 Groundwater drought in the northwestern districts of Bangladesh. *Water Resources Management* **24**, 1989–2006. https://doi.org/10.1007/s11269-009-9534-y.

Sharma, K. D. 1998 The hydrological indicators of desertification. *Journal of Arid Environment* **39** (2), 121–132. https://doi.org/10.1006/jare.1998.0403.

Simmers, I. 1997 *Recharge of Phreatic Aquifers in (Semi-) Arid Areas*. International Ass. Hydrogeol. 19, A.A. Balkema, Rotterdam, 227 p.

Sophocleous, M. A. & Delvin, J. F. 2004 Discussion of 'The water budget myth revisited: Why hydrogeologists model' by John D. Bredehoeft. *Ground Water* **42**, 618. 10.1111/j.1745-6584.2004.tb02630.x.

Tan, M. L., Samat, N., Chan, N. W., Lee, A. J. & Li, C. 2019 Analysis of precipitation and temperature extremes over the Muda River Basin, Malaysia. *Water* **11**, 283. https://doi.org/10.3390/w11020283.

Teklebirhan, A., Dessie, N. & Tesfamichael, G. 2012 Groundwater recharge, evapotranspiration and surface runoff estimation using WetSpass modeling method in Illala catchment, Northern Ethiopia. *Momona Ethiopian Journal of Science* **4** (2), 96–110. https://doi: 10.4314/mejs.v4i2.80119.

Tesfamichael, G., De Smedt, F., Walraevens, K., Gebresilassie, S., Hussien, A., Hagos, M. & Gebrehiwot, K. 2013 Application of a spatially distributed water balance model for assessing surface water and groundwater resources in the Geba Basin, Tigray, Ethiopia. *Journal of Hydrology* **499**, 110–123.

UN/WWAP (United Nations/World Water Assessment Programme) 2006 *UN World Water Development Report 2. Water a shared Responsibility*. United Nations Educational, Scientific and Cultural Organization, Paris. France and Berghahn Books, New York, USA, 600 p.

Voss, K. A., Famighlietti, J. S., Lo, M. H., Linage, C., Rodell, M. & Swenson, S. C. 2013 Groundwater depletion in the Middle East from GRACE with implication for trans boundary water management in the Tigris-Euphrates-Western Iran Region. *Water Resource Research* **49** (2), 904–914. doi:10.1002/wrcr.20078.

Wang, W., Wei, J., Shao, Q., Xing, W., Yong, B., Yu, Z. & Jiao, X. 2015 Spatial and temporal variations in hydro-climatic variables and runoff in response to climate change in the Luanhe River basin, China. *Stochastic Environmental Research and Risk Assessment* **29**, 1117–1133. https://doi.org/10.1007/s00477-014-1003-3.

Xu, Y. 2011 Book review: Estimating groundwater recharge, by Richard W Healy (Cambridge University Press, 2010). *Hydrogeology Journal* **19**, 1451–1452. https://doi.org/10.1007/s10040-011-0764-8.

Yongxin, X. & Beekman, H. E. 2003 *Groundwater's Recharge Estimation in Southern Africa*. United Nations Educational Scientific and Cultural Organization, Paris. UNESCO IHP Series No. 64. 206 P. ISBN 92-9220-000-3.

Zeabraha, A., G/yohannes, T., W/Mariyam, F., Mulugeta, A. & Gebreyesus, Z. 2020 Application of a spatially distributed water balance model for assessing surface and groundwater resources: A case study of Adigrat area, Northern Ethiopia. *Sustainable Water Resources Management* **6**, 73. https://doi.org/10.1007/s40899-020-00424-5.

First received 7 August 2023; accepted in revised form 18 January 2024. Available online 2 February 2024